

Supporting Information

Multisource energy conversion in plants with soft epicuticular coatings

*Fabian Meder**, *Alessio Mondini*, *Francesco Visentin*, *Giorgio Zini*, *Marco Crepaldi*, *Barbara Mazzolai**

Figure S1. Circuit model used to estimate the behavior of two leaf generators on the same or separate plants.

Figure S2. Effect of the leaf coating on self-healing of wounded leaves.

Figure S3. Mechanical energy conversion by c-u leaf pairs.

Figure S4. Scanning electron microscopy images of the coated *H. helix* leaves and effect of coating thickness on the voltage output.

Figure S5. Mechanical-to-electrical energy conversion efficiency of a c-u leaf pair.

Figure S6. Influence of climber *H. helix*' support material on the mechanical energy conversion.

Figure S7. Model for the estimation of the behavior of signal generation and energy harvesting with multiple leaves on the same plant.

Figure S8. Influence of leaf-wetting on c-u leaf pair energy conversion.

Figure S9. Electric field characteristics and field strength-dependent energy harvesting using *H. helix*.

Figure S10. Effect of ion conduction obstruction by tissue drying on energy harvesting and impedance analysis.

Figure S11. Application scenario: Signals received during plant-based RF energy harvesting in an urban outdoor environment.

Table S1. Overview of plant-hybrid energy harvesting and sensing techniques.

Movie 1. Cable-free, leaf tangency-enabled wind energy conversion by living plants

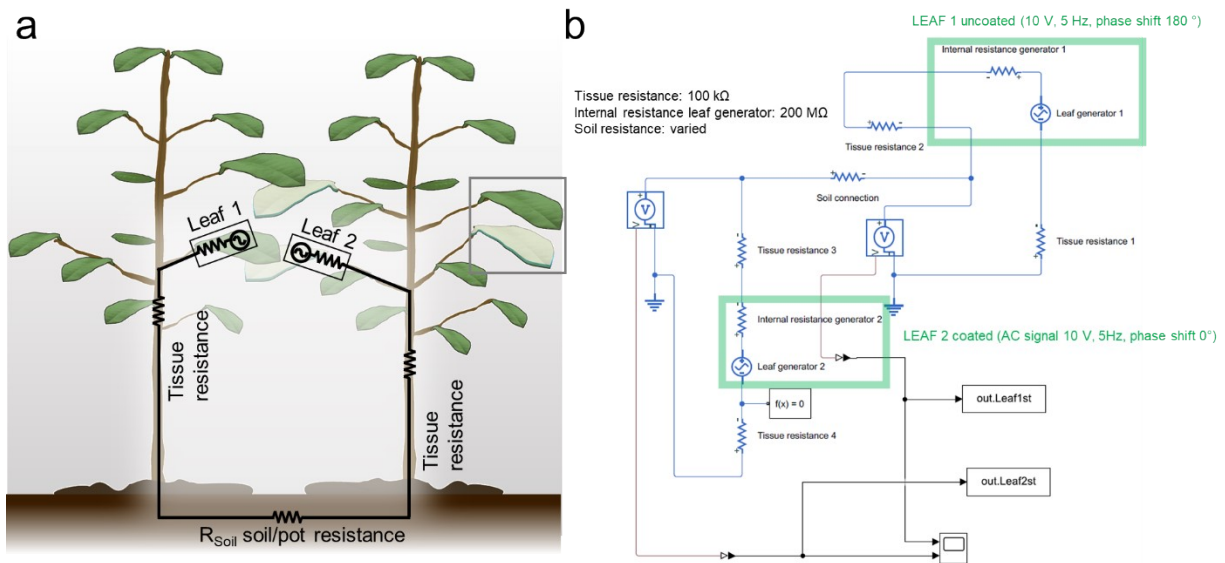


Figure S1. Circuit model used to estimate the behavior of two leaf generators on the same or separate plants. a) Illustration of the circuit model with two plants as in Figure 1 of the main article. b) Schematic of the implementation of the circuit simulation in Simulink to obtain the estimation of the behavior of the leaf generators given in Figure 1c and 1d of the main article.

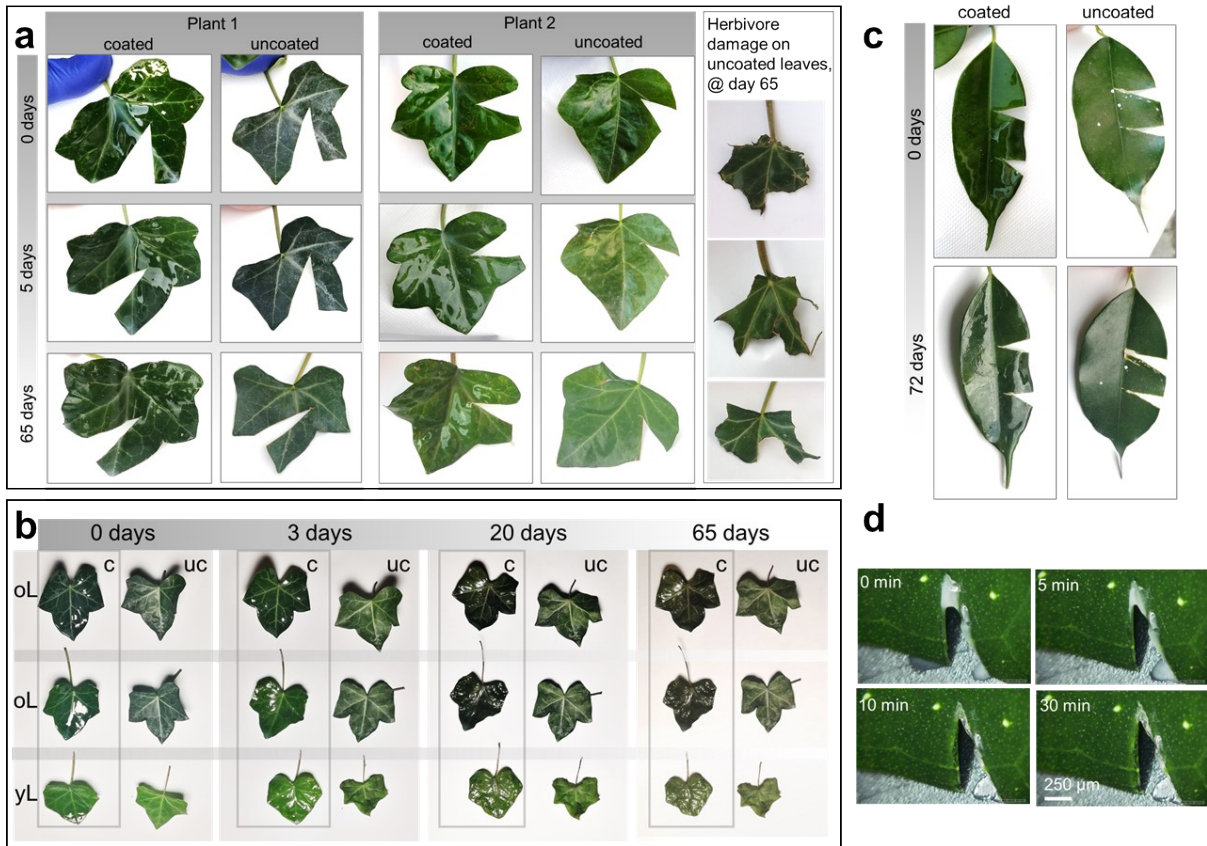


Figure S2. Effect of the leaf coating on self-healing of wounded leaves. a) Coated and uncoated *H. helix* leaves of the same plant observed for a period of 65 days after wounding by cutting out a V-shaped piece of the leaf. The wounded leaves remained on the plant which was kept outdoor for the indicated periods. Both, coated and uncoated leaves survived the wounding with no visible signs of a loss of functionality. The panel on the right shows an herbivore damage which occurred during the experimental period only on uncoated leaves. This suggests that the elastomeric coating does not affect wound healing and may, moreover, have a protective effect against wounding. b) Effect of the coating of *H. helix* leaves on the process of wilting after the leaves (oL: old leaves, yL: young leaves) were removed from the plant and subsequently observed for 65 days. A clear color change and wrinkling of both, coated and uncoated leaves can be seen which was not observed when the leaves were kept alive on the plant. c) Effect of coating on recovery from wounding in a *Ficus benjamina* for which self-repair mechanism by coagulation of plant sap latex is well

known.⁴¹ The experiments show that both, coated and uncoated leaves self-heal and remain alive. d) Microscopy of the latex coagulation of a coated leaf within 30 min after wounding. All experiments clearly confirmed that coated leaves overcome a wounding event similar to uncoated leaves and that thus the coating does not reduce the leaves' survival. Instead, it may even have a protective effect against wounding by, e.g., herbivores. Self-healing was tested on 5 leaves of the same plant per condition (coated/uncoated) treated in the same manner, the results give representatives images.

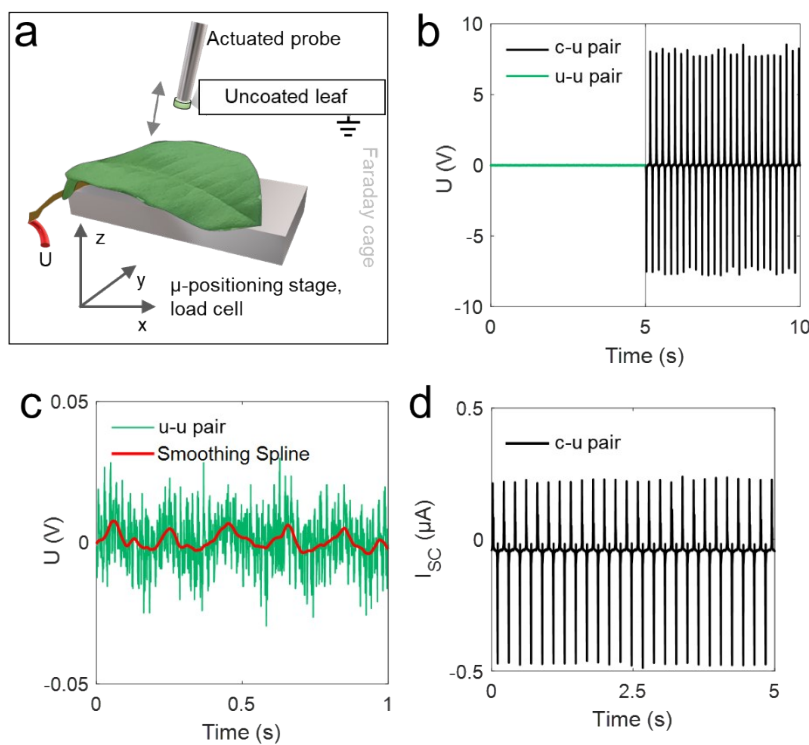


Figure S3. Mechanical energy conversion by c-u leaf pairs. a) Schematic of the setup for applying controlled mechanical stimuli between a circular section of an uncoated and uncoated or coated and uncoated leaf, respectively to establish u-u and c-u pairs. b) Alternating voltage signals generated by a c-u pair of *F. microcarpa* @ 5 Hz, 1 N stimulus showing significant enhancement of output voltage after epicuticular coating. c) Zoom-in of

the voltage signal generated by the u-u pair with an amplitude of ~ 45 mV. The smoothing spline reveals the 5 Hz stimulus signal. The amplitude of the c-u pair is thus ~ 450 times higher as achieved by the u-u pair. d) Short circuit current generated by a c-u pair of *F. microcarpa* @ 5 Hz, 1 N stimulus.

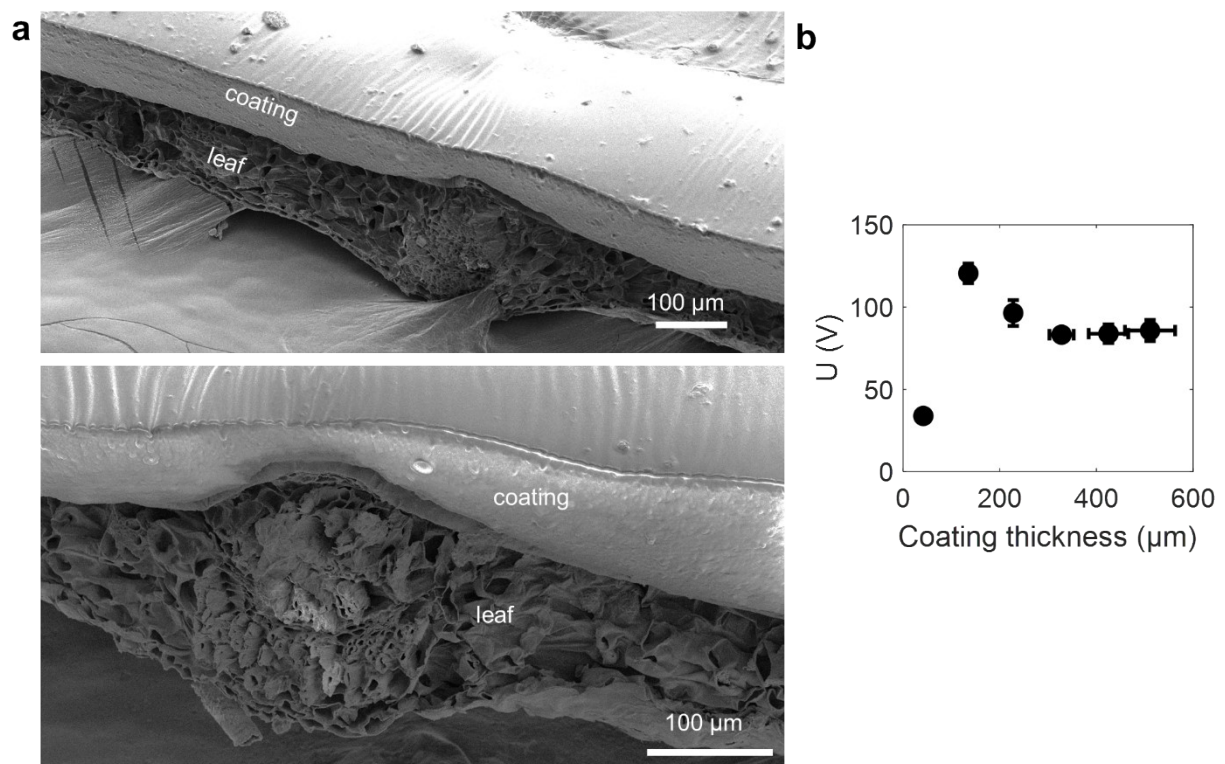


Figure S4. Scanning electron microscopy images of the coated *H. helix* leaves and effect of coating thickness on the voltage output. a) Scanning electron microscopy images of sections of *H. helix* leaves after coating of the epicuticular region with silicone elastomers. The images show that the coating is conformably attached to the leaf surface. b) Effect of the coating thickness on the voltage produced by a c-u leaf pair. During the tests, mechanical stimulation (1 N, 5 Hz, 1 cm^2 contact area) between the coated and uncoated leaf was applied by an actuator in a Faraday cage and the voltage was measured between electrodes inserted in the petiole of the two leaves. The x and y error bars represent average and

standard deviation of six leaves subject to 150 contacts and six different coating thicknesses (a total of 900 tests). The results suggest that there is an optimum of the coating thickness (here 135 μm) that, under the conditions of the experiments, leads to highest voltage generation (up to 120 V). The increase could be related to the dielectric properties but also to an optimal softness and adaptation to the contact surface. Controlling coating thickness could thus be used further tune the output of the c-u leaf pairs.

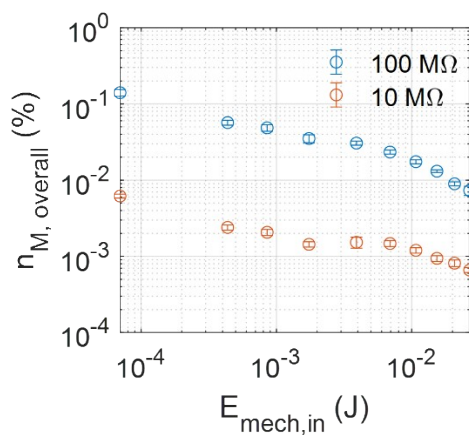


Figure S5. Mechanical-to-electrical energy conversion efficiency of a c-u leaf pair. A certain mechanical energy $E_{\text{mech,in}}$ was applied to a c-u leaf pair of *H. helix* by a pendulum as described in the methods section and the resulting electrical energy produced was determined from the current measured over a 10 or 100 M Ω resistor, respectively. The results show that the leaves' mechanical-to-electrical energy conversion efficiency $n_{M, \text{overall}}$ varies within a magnitude dependent on the kinetic energy introduced. It was found higher at lower input energy reaching values of up to 0.14 %. A reason for this behavior could be that energy conversion efficiency is a function of the impact force which increases at higher $E_{\text{mech,in}}$ and has an maximum at a given force as suggested earlier.³⁶ Each datapoint represents mean and standard deviation of 3 individual c-u pairs that were tested by 6 current measurement per $E_{\text{mech,in}}$ (total of 360 measurements).

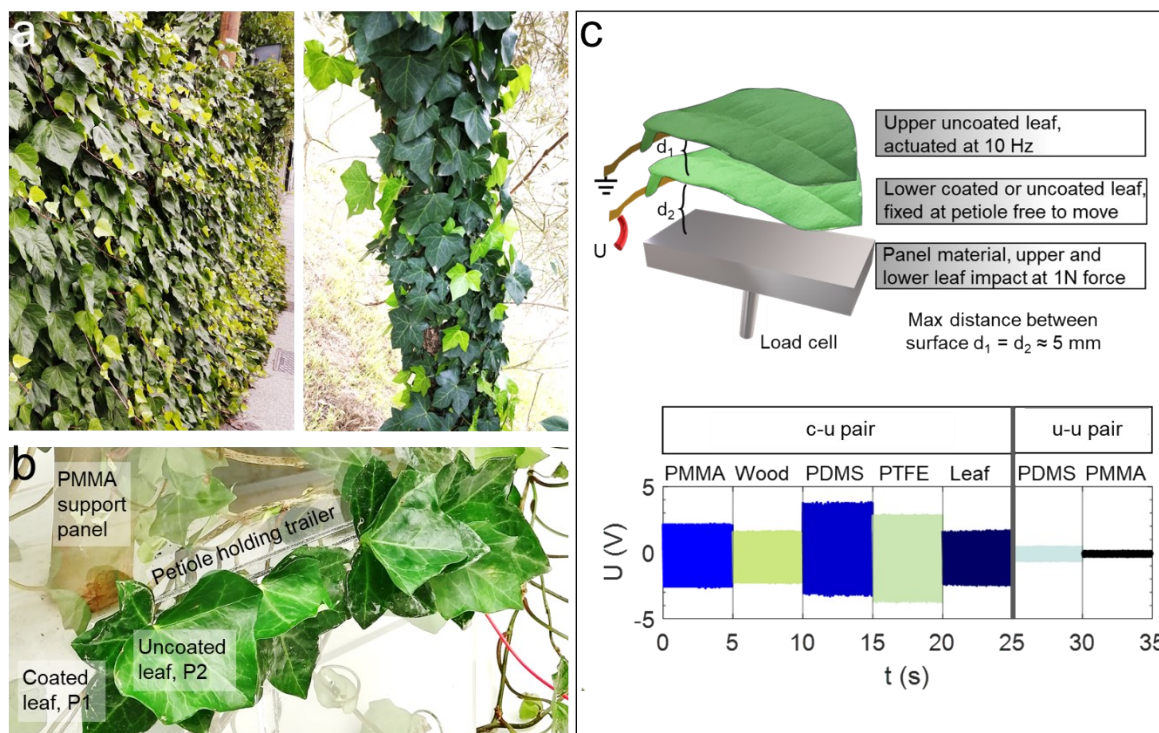


Figure S6. Influence of climber *H. helix*' support material on the mechanical energy conversion. a) *H. helix* typically grows and climbs on a rigid support such as a wall or tree leading to multiple overlapping leaves from several branches. The support also introduces a barrier for mechanical motion of the leaf in the wind reducing the degrees of freedom for elastic deformation and increasing mechanical contact for energy conversion between the overlapping leaves. c) Image of the PMMA support panel used for wind-exposure experiments in which multiple leaves of two branches of two *H. helix* plants (one coated, one uncoated) can be fixed at the petiole creating a c-u pair free to move in the wind while being connected to the main plant and supported by the PMMA panel. c) We tested how the material used as support influences the voltage generation. The depicted arrangement was employed in which an uncoated leaf was actuated onto a coated/uncoated leaf kept at a given distance from a support material. The graph below shows the generated voltage signals (10 Hz stimulus) using PMMA, wood, PDMS, PTFE, and another leaf as support

material when analyzing c-u and u-u pairs. PDMS and PTFE enhance the signal which can be explained by an additional contact charging due to contact of the leaf with this surface. PMMA, wood, and leaf as a substrate does not significantly change the signal. Using the u-u pair, the signal is expectedly lower and only slightly increased by the substrate and the main contribution for generated voltage is the c-u and u-u leaf pair.

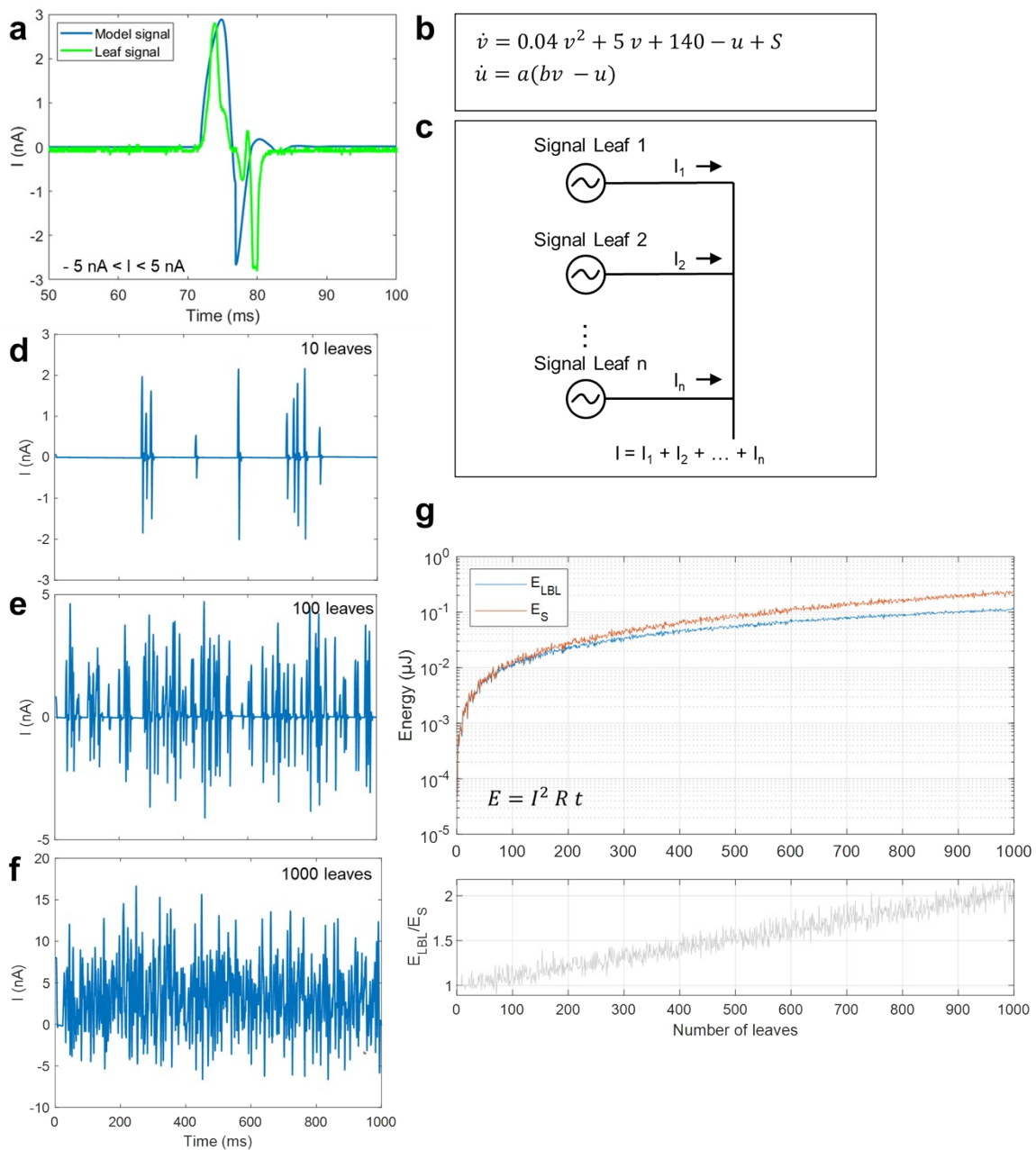


Figure S7. Model for the estimation of the behavior of signal generation and energy

harvesting with multiple leaves on the same plant. a) The figure shows the comparison between the typical AC current signals generated by a c-u leaf contact (experimental data, green curve) and a mathematical description of this current signals derived using the equations given in b) (blue curve). b) Model equations by Izhikevich³⁵ that were used to describe the current spikes generated by a c-u leaf contact where v , u , S , a and b , respectively are variables to tune the spike width, magnitude, and positive/negative components. c) Circuit model of a plant with n leaves connected through the tissue and producing current signals at random timings. In this simplified estimation, we assume that Kirchhoff's current law applies and the final current that can be harvested with an electrode in the tissue I corresponds to the sum of the currents generated by the individual leaves $I_1+I_2+...+I_n$. d), e), and f) show current spikes obtained by our model using either 10, 100, or 1000 leaves, respectively randomly generating signals within a timeframe of 1000 ms. The signals were generated in the limits of $-5 \text{ nA} \leq I \leq +5 \text{ nA}$ and it can be seen that for 1000 leaves, the current spikes overcome these limits by the event that multiple spikes occurring at the same time sum up. g) The upper panel shows the cumulative sum of the energy E over the measurement period with t being the data acquisition period and R being the inner resistance of the plant-hybrid generator with a value of $200 \text{ M}\Omega$ as determined by our measurements. E_{LBL} gives the cumulative energy considering each spike independently (each leaf individual and not connected to the other leaves through the tissue). E_S instead describes the cumulative energy after current signals summed up according to Kirchhoff's law. The lower panel shows the quotient of E_S and E_{LBL} . The results show that the E_S and E_{LBL} behave in general similar and are equivalent up to ~ 80 leaves. There is a clear increase in E_S when more leaves are used, maximal twice the value of E_{LBL} . When currents sum up the

negative and the positive components of the signals will compensate but the model shows that there is still a positive sum current (as also confirmed by our experiments with up to eight leaves, Figure 4j). The cumulative energy could be even higher than when each signal could be harvested individually as positive peaks occurring simultaneously sum up as well. Moreover, the estimation shows that E in both cases increases the more leaves are used. This suggests that upscaling using multiple leaves that produce signals on the same plant could expectedly be possible. This suggests that upscaling using multiple leaves that produce signals on the same plant expectedly is possible. Our experimental results with eight leaves (Figure 4j and 5f) show a positive power balance and signals did not cancel out. Yet, the model should be confirmed by further experimental results with larger amounts of leaves. Limitations of the model that require experimental observations are for example the fact that leaves on the same branch often undergo similar mechanical constraints that lead to similar and potentially to motion which is to some extent synchronized. Hence signals from multiple leaves would not appear randomly but moderately synchronized which could further improve the power balance by reducing the event that a positive spike hits a negative spike of another leaf leading to canceling out of the signals. Furthermore, the circuit model needs to be extended by including factors like capacitances of the tissue or different internal resistances for the individual leaf generators. Yet, plant-based harvesters using a few leaves presented here can already power commercial electronics like wireless sensor nodes. Further upscaling and optimizing the model as well as the energy outputs is part of our future investigation.

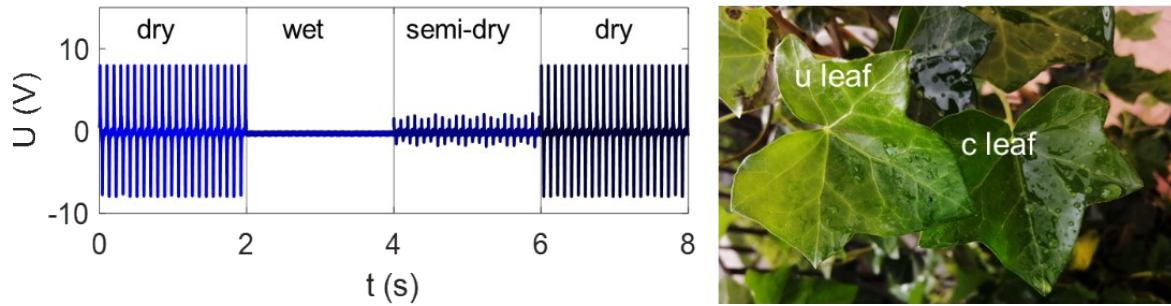


Figure S8. Influence of leaf-wetting on c-u leaf pair energy conversion. A *H. helix* c-u leaf pair was exposed to a 10 Hz mechanical stimulus and voltage amplitude is recorded before and after wetting the leaves by spraying water. Wetting expectedly strongly reduces contact electrification and the obtained voltage amplitudes. However, the signal recovers when the leaves dry again.

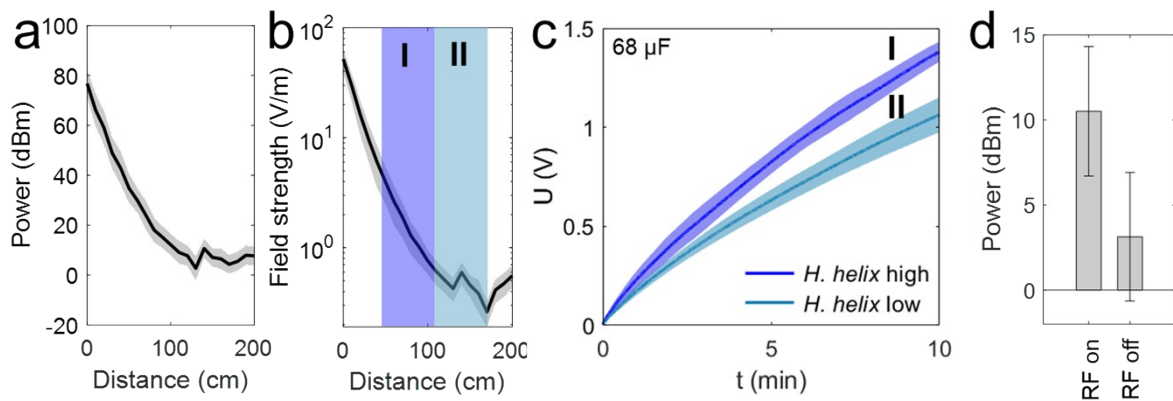


Figure S9. Electric field characteristics and field strength-dependent energy harvesting using *H. helix*. a) and b) power and field strength as function of distance of RF source. The results are mean and standard deviation (filled grey area behind curve) of 350 measurements performed within an acquisition time of 90 seconds. Power and field strength were measured of 20 different distances were measured varied in 10 cm steps. c) 68 μF capacitor charging with *H. helix* when placed in different distances from the RF source corresponding to the blue (I.) and green (II.) area in b). The curves are averages from 4 to 7 repetitions per measurement conditions, the filled areas behind the curves represent the

standard deviation. For some measurements the standard deviation is about the linewidth.

d) Difference in the average power of the electric field measured when RF source (fluorescent lighting system) is switched on/off. The bars show mean and standard deviation of seven individual measurements for each condition.

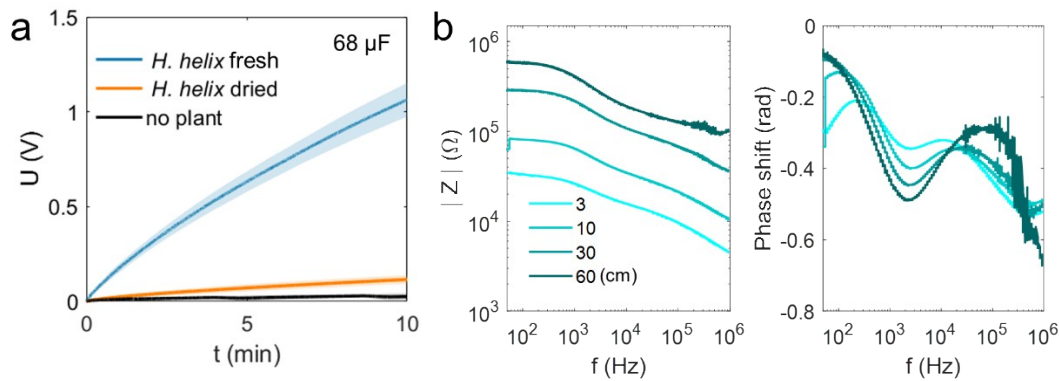


Figure S10. Effect of ion conduction obstruction by tissue drying on energy harvesting and impedance analysis. a) Influence of the *H. helix* water content on RF energy conversion and capacitor charging. Naturally drying the tissue (by omitting watering for 4 weeks, orange curve) obstructs ion conduction and results in an almost complete loss of charging compared to the fresh *H. helix* (blue curve) indicating that tissue water content and related ion mobility in living plants is expectedly essential for RF energy conversion and harvesting. The curves are averages from 3 to 7 repetitions per measurement conditions, the filled areas behind the curves represent the standard deviation. For some measurements the standard deviation is about the linewidth. b) Bode plots of impedance $|Z|$ and phase shift of a *H. helix* branch as function of the length given in cm (branch diameter ~ 5 mm).

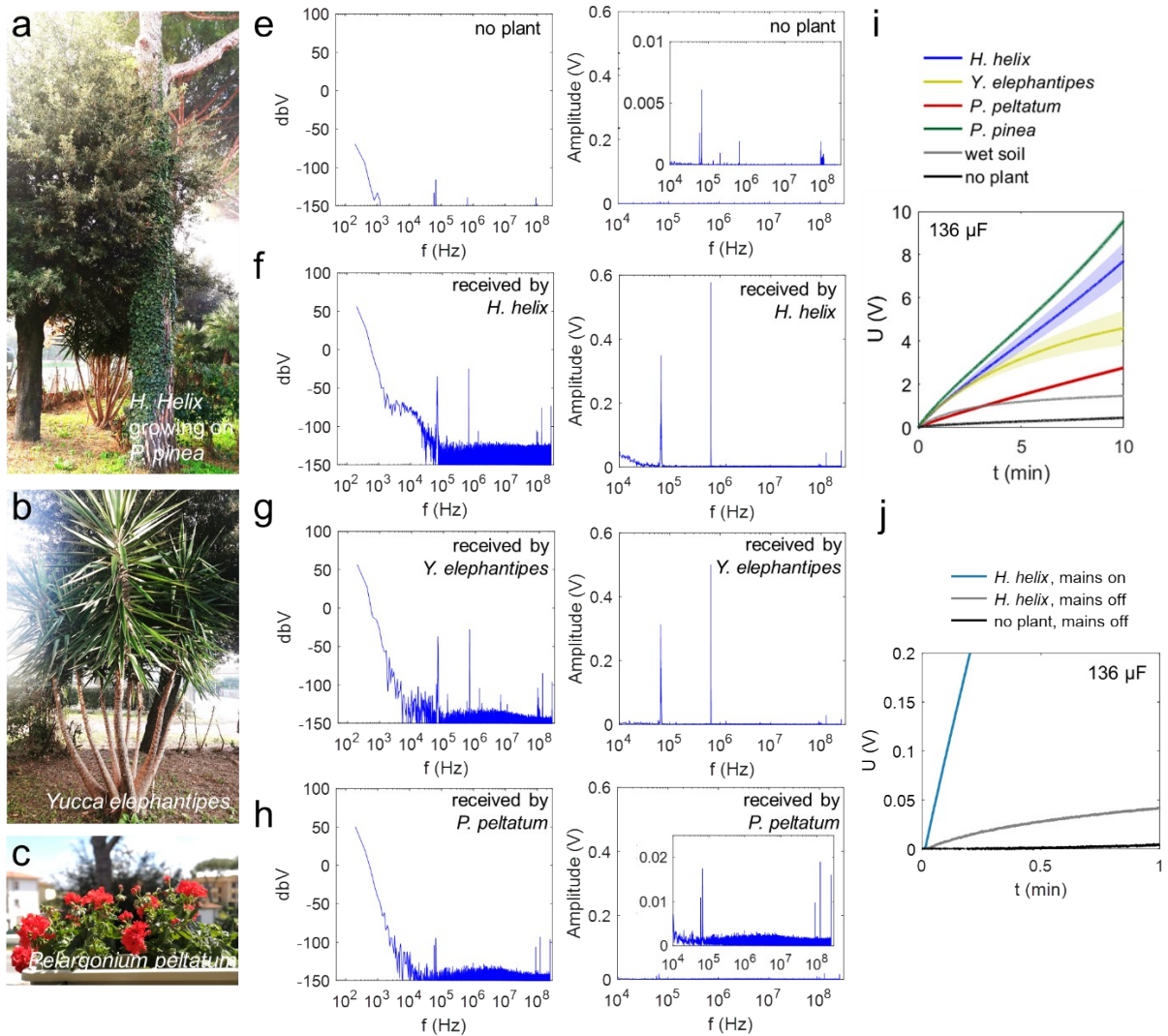


Figure S11. Application scenario: Signals received during plant-based RF energy harvesting in an urban outdoor environment. a) to c) images of the different species used for energy harvesting in a front garden and on a balcony of a multifamily residence. e) to h) Hanning-windowed frequency spectrum analysis (dbV, full range, left; V, >10 kHz, right) of voltage signals received by different plants (*H. helix*, *Y. elephantipes*, and *P. peltatum*). The house' ground was used as reference point/potential difference. Insets are zoom-ins into smaller peaks of the spectrum. Plants strongly increase the signal reception at multiple frequencies starting from super low mains noise to the GHz range. Spectrum analysis of *H. helix* and *Y. elephantipes* shows among other frequencies also the clearly distinguishable signals of a nearby 657 kHz MW radio emitter (8 km distance). i) Plant-dependent charging dynamics of

a 136 μF capacitor. Measurement in wet soil (an electrode was inserted 20 cm instead of the plant) and with no plant connected, respectively were performed as reference. *P. pinea* results in highest instantaneously transferred power of $\sim 10 \mu\text{W}$ and *H. helix* delivers $6.8 \mu\text{W}$, *P. peltatum* results in $0.8 \mu\text{W}$. The plant-dependent output behavior is likely due to the plant size and branching that forms the receiving antenna. The curves are averages of 3 repetitions per plant species, the filled areas behind the curves represent the standard deviation. For some measurements the standard deviation is about the linewidth. j) Analysis of 136 μF capacitor charging dynamics by *H. helix* when the mains circuit of the near-by multifamily residence is turned off, revealing that the energy output is strongly affected by the building mains.

Table S1. Overview of recent plant-hybrid energy harvesting and sensing techniques. a) Examples of techniques to harvest electrical energy that use plants as part of the devices. The table gives an overview of approaches in the literature, their principles, the power measures, examples for what the energy was used, and an indication if the systems were tested outdoors and compares it with this work. b) Overview of other recent plant-hybrid technologies that allow to sense and transmit data from the plants to external devices or directly produce light with plants. For a more complete overview, the reader is referred to references ^{15–18}.

a) Electrical energy harvesting by plants				
Principle	Reported power measures	Used to	Outdoor tests performed	Reference
Mechanical energy conversion with artificial leaves installed on natural leaves	$15 \mu\text{W}/\text{cm}^2$ contact area, up to 150 V (max)	Powering LEDs	No	¹
Mechanical energy harvesting with leaves	$4.5 \mu\text{W}/\text{cm}^2$ contact area, up to 240V (max)	Powering LEDs	No	²

Wind energy harvesting with leaves	143 nW	Powering LEDs and temperature sensor	Yes	23
This work - mechanical/wind energy harvesting by coated leaves	17 $\mu\text{W}/\text{cm}^2$ contact area, up to 150 V (max), 0.26 μW , 10 V under wind excitation	Powering LEDs, wireless temperature/humidity sensor	No	This work
This work - RF energy harvesting by leaves	Between 0.25 μW and 10 μW were achieved with different RF sources and species	Powering wireless temperature/humidity sensor	Yes	This work
Glucose- O_2 bio fuel cell in a grape	2.4 μW , 0.54 V		No	30
Enzymatic biofuel cell in grapes	6.3 μW at 0.25 V	Monitoring sugar levels in fruits	No	29
Plant microbial fuel cell at roots/soil	22.2 $\mu\text{W}/\text{cm}^2$ electrode area, up to 0.4V		No	25
Plant microbial fuel cell at roots/soil	32 $\mu\text{W}/\text{cm}^2$ electrode area	Signal amplifier for 5G wireless networks	No	27
Temperature gradients using Peltier cell in the trunk	112 μW , up to 0.08 V (max)	Powering wireless sensor nodes	Yes	31
Potential difference between electrodes in a tree trunk and in the soil	10 nW	A boost circuit and a low frequency timer	Yes	32

b) Plant-hybrid systems that do not directly produce electricity but emit light or enable sensing				
Purpose	Principle	Outcomes/signal acquisition/signal transmission	Used to	Reference
Light emission	Engineered nanoparticles in leaves to introduce firefly luciferase–luciferin reaction utilizing ATP to emit light	Light emitting living plant tissue	Producing light, photon emission ~50% of 1 μW commercial luminescent diodes	19
Sensing	Single-walled carbon nanotubes (SWCNTs) conjugated to a peptide embedded in leaf mesophyll	Remote near-infrared fluorescence monitoring	Measure nitroaromatics in soil and ground water and communication to smartphone	7
Sensing	Single-walled carbon nanotubes (SWCNTs) in chloroplasts	Remote near-infrared fluorescence monitoring	Nitric oxide sensor	9
Sensing	Single-walled carbon nanotubes (SWCNTs) in leaf tissue	Remote near-infrared fluorescence	Arsenic detection	11

		monitoring		
Sensing	Single-walled carbon nanotubes (SWCNTs) in leaf tissue	Remote near-infrared fluorescence monitoring	H ₂ O ₂ monitoring	¹³
Sensing	enzymatic biosensors based on organic electrochemical transistors in the vascular tissue of trees	Voltage readout	glucose and sucrose monitoring	¹⁴
Sensing	Polymer tattoo electrodes on leaves	Impedance measurements	ozone damage in plants	¹⁰
Sensing and growth manipulation	Hydroprinted liquid-alloy-based morphing surface of leaves;[11] deposited thin gold electronics	Resistance measurements and integrated LEDs to manipulate growth	monitor leaf moisture content and length, and manipulate leaf and bean sprout orientation	¹²